A hybrid tool for spectral ray tracing simulations of luminescent cascade systems

Sven Leyre,[1,2,3,*] Jana Ryckaert,[1] Paula Acuña,[1] Jan Audenaert,[1] Youri Meuret,[1] Guy Durinck,[1] Johan Hofkens,[4] Geert Deconinck,[2] and Peter Hanselaer[1]

[1]*ESAT/Light & Lighting Laboratory, KU Leuven, Gebroeders Desmetstraat 1, Gent, 9000, Belgium*
[2] *ESAT/ELECTA, KU Leuven, Kasteelpark Arenberg 10, bus 2445, 3001 Leuven, Belgium*
[3]*SIM (Flemish Strategic Initiative on Materials), SOPPOM program, Technologiepark 935, 9052 Zwijnaarde, Belgium*
[4]*Departement of Chemistry, KU Leuven, Celestijnenlaan 200 F, bus 2404, Leuven 3001, Belgium*
[*]*Sven.Leyre@kuleuven.be*

Abstract: To perform adequate simulations of luminescent cascade systems, a hybrid method combining a commercial ray tracer and a programming tool is presented. True Monte Carlo algorithms for luminescent materials, treating each ray individually, are adapted to allow wavelength conversion of ray sets. Two solutions for the wavelength conversion of ray sets are discussed: a random approach, where absorption events are randomly selected to create emission events, and a combined approach, where information from multiple absorption events is combined to create emission events. Both methods are applied to simulate the performance of a virtual remote phosphor light-emitting diode module. When using the combined approach, the required computation time to achieve sufficient accuracy is a factor 2 lower, compared to the time required when applying the random approach.

OCIS codes: (080.2740) Geometric optical design; (160.2540) Fluorescent and luminescent materials.

References and links

1. T. Ritschel, C. Dachsbacher, T. Grosch, and J. Kautz, "The state of the art in interactive global illumination," Comput. Graph. Forum **31**(1), 160–188 (2012).
2. M. Vinkler, J. Bittner, V. Havran, and M. Hapala, "Massively parallel hierarchical scene processing with applications in rendering," Comput. Graph. Forum **32**(8), 13–25 (2013).
3. A. Liebert, H. Wabnitz, N. Zołek, and R. Macdonald, "Monte Carlo algorithm for efficient simulation of time-resolved fluorescence in layered turbid media," Opt. Express **16**(17), 13188–13202 (2008).
4. A. J. Welch, C. Gardner, R. Richards-Kortum, E. Chan, G. Criswell, J. Pfefer, and S. Warren, "Propagation of fluorescent light," Lasers Surg. Med. **21**(2), 166–178 (1997).
5. L. Wang, S. L. Jacques, and L. Zheng, "MCML—Monte Carlo modeling of light transport in multi-layered tissues," Comput. Meth. Prog. Bio. **47**(2), 131–146 (1995).
6. C. Zhu and Q. Liu, "Review of Monte Carlo modeling of light transport in tissues," J. Biomed. Opt. **18**(5), 050902 (2013).
7. J. Audenaert, F. B. Leloup, B. Van Giel, G. Durinck, G. Deconinck, and P. Hanselaer, "Impact of the accurateness of bidirectional reflectance distribution function data on the intensity and luminance distributions of a light-emitting diode mixing chamber as obtained by simulations," Opt. Eng. **52**(9), 095101 (2013).
8. S. C. Shen, C. Y. Kuo, and M.-C. Fang, "Design and analysis of an underwater white LED fish-attracting lamp and its light propagation," Int. J. Adv. Robot. Syst. **10**, 183 (2013).
9. J. Audenaert, G. Durinck, F. Vandeghinste, G. Deconinck, and P. Hanselaer, "Feasibility study of a brute-force ray tracing approach to obtain luminance maps of luminaires modeled with ray files," Proc. SPIE **7717**, 77170L (2010).
10. Z.-M. Zhu, X.-L. Jin, H. Yang, and L.-S. Zhong, "Design of diffuse reflection freeform surface for uniform illumination," J. Display Technol. **10**(1), 7–12 (2014).
11. R. Hu, X. Luo, and H. Zheng, "Hotspot location shift in the high-power phosphor-converted white light-emitting diode packages," Jpn. J. Appl. Phys. **51**, 09MK05 (2012).
12. W. Y. Lee, T. K. Lim, Y. W. Lee, and I. W. Lee, "Fast ray-tracing methods for LCD backlight simulation using the characteristics of the pattern," Opt. Eng. **44**(1), 014004 (2005).
13. B. Van Giel, Y. Meuret, L. Bogaert, H. Murat, H. De Smet, and H. Thienpont, "LED projector with two liquid crystal on silicon light valves and a fly's eye integrator," Displays **29**(5), 464–470 (2008).

#217365 - $15.00 USD Received 18 Jul 2014; revised 20 Sep 2014; accepted 23 Sep 2014; published 30 Sep 2014

14. P. C.-P. Chao, C.-H. Tsai, J.-D. Li, and W.-D. Chen, "Optimizing angular placements of the LEDs in a LCD backlight module for maximizing optical efficiency," Microsyst. Technol. **19**(9–10), 1669–1678 (2013).
15. B. S. Richards and K. R. McIntosh, "Overcoming the poor short-wavelength spectral response of CdS/CdTe photovoltaic modules via luminescence downshifting: ray-tracing simulations," Prog. Photovolt. Res. Appl. **15**(1), 27–34 (2007).
16. W. G. J. H. M. Van Sark, K. W. J. Barnham, L. H. Slooff, A. J. Chatten, A. Büchtemann, A. Meyer, S. J. McCormack, R. Koole, D. J. Farrell, R. Bose, E. E. Bende, A. R. Burgers, T. Budel, J. Quilitz, M. Kennedy, T. Meyer, C. M. Donegá, A. Meijerink, and D. Vanmaekelbergh, "Luminescent Solar Concentrators--A review of recent results," Opt. Express **16**(26), 21773–21792 (2008).
17. S. W. Leow, C. Corrado, M. Osborn, and S. A. Carter, "Monte Carlo ray-tracing simulations of luminescent solar concentrators for building integrated photovoltaics," Proc. SPIE **8821**, 882103 (2013).
18. D. Şahin, B. Ilan, and D. F. Kelley, "Monte-Carlo simulations of light propagation in luminescent solar concentrators based on semiconductor nanoparticles," J. Appl. Phys. **110**(3), 033108 (2011).
19. A. Schüler, A. Kostro, B. Huriet, C. Galande, and J.-L. Scartezzini, "Monte Carlo simulations of quantum dot solar concentrators: ray tracing based on fluorescence mapping," Proc. SPIE **7046**, 704609 (2008).
20. D. Şahin and B. Ilan, "Radiative transport theory for light propagation in luminescent media," J. Opt. Soc. Am. A **30**(5), 813–820 (2013).
21. L. H. Slooff, A. R. Burgers, and E. Bende, "The luminescent solar concentrator: a parameter study towards maximum efficiency," Proc. SPIE **7002**, 700209 (2008).
22. S. Leyre, J. Cappelle, G. Durinck, A. Abass, J. Hofkens, G. Deconinck, and P. Hanselaer, "The use of the adding-doubling method for the optical optimization of planar luminescent down shifting layers for solar cells," Opt. Express **22**(S3 Suppl 3), A765–A778 (2014).
23. S. Dhami, A. J. de Mello, G. Rumbles, S. M. Bishop, D. Phillips, and A. Beeby, "Phthalocyanine fluorescence at high concentration: dimers or reabsorption effect?" Photochem. Photobiol. **61**(4), 341–346 (1995).
24. Á. Borbély and S. G. Johnson, "Performance of phosphor-coated light-emitting diode optics in ray-trace simulations," Opt. Eng. **44**(11), 111308 (2005).
25. T. J. J. Meyer, J. Hlavaty, L. Smith, E. R. Freniere, and T. Markvarta, "Ray racing techniques applied to modelling of fluorescent solar collectors," Proc. SPIE **7211**, 72110N (2009).
26. C. Sommer, F.-P. Wenzl, P. Hartmann, P. Pachler, M. Schweighart, S. Tasch, and G. Leising, "Tailoring of the color conversion elements in phosphor-converted high-power LEDs by optical simulations," IEEE Photon. Technol. Lett. **20**(9), 739–741 (2008).
27. R. Hu, S. Yu, Y. Zou, H. Zheng, F. Wang, S. Liu, and X. Luo, "Near-/mid-field effect of color mixing for single phosphor-converted light-emitting diode package," IEEE Photon. Technol. Lett. **25**(3), 246–249 (2013).
28. P. Acuña, S. Leyre, J. Audenaert, Y. Meuret, G. Deconinck, and P. Hanselaer, "Power and photon budget of a remote phosphor LED module," Opt. Express **22**(S4 Suppl 4), A1079–A1092 (2014).
29. Z. Liu, S. Liu, K. Wang, and X. Luo, "Measurement and numerical studies of optical properties of YAG:Ce phosphor for white light-emitting diode packaging," Appl. Opt. **49**(2), 247–257 (2010).
30. W.-S. Song, S.-H. Lee, and H. Yang, "Fabrication of warm, high CRI white LED using non-cadmium quantum dots," Opt. Mater. Express **3**(9), 1468–1473 (2013).

1. Introduction

Accurate ray tracing simulations are of interest for a broad range of applications, such as computer graphics [1,2], diagnostic tools in the bio-medical field [3–6], and optical design tools for luminaires [7–11], displays [12–14], and photovoltaic devices [15–22]. When considering systems including luminescence, ray tracing software has extensively been used for the modeling of phosphor converted white light-emitting diodes (pcLEDs), luminescent solar concentrators (LSCs), and solar cell planar luminescent down-shifting layers to enhance the spectral response at short wavelengths.

In "true" Monte Carlo ray tracing simulations, photoluminescence is considered for each ray (or photon) individually. After being absorbed in a luminescent component, a new ray with a wavelength lying within the emission spectrum of the material is generated, with a probability equal to the quantum yield of the luminescent material. This approach allows a ray to be absorbed and re-emitted multiple times. This is essential for the modelling of luminescent cascade systems. In these systems, multiple luminescent materials of which the absorption spectrum of one material overlaps with the emission spectrum of another material, are combined. Even when dealing with only one luminescent material with a significant overlap between the excitation and emission spectra, re-absorption and re-emission processes are important and have to be included [23].

When dealing with simple optical systems, straight forward programming of true Monte Carlo algorithms is possible. A typical example of such systems is an LSC [17–21]. In an LSC sunlight is incident on a transparent sheet containing one or more luminescent dyes, which partially absorb the incident photons and isotropically re-emit photons with a longer

#217365 - $15.00 USD Received 18 Jul 2014; revised 20 Sep 2014; accepted 23 Sep 2014; published 30 Sep 2014

wavelength. Due to total internal reflection at the top and bottom of the sheet, photons travel towards the side edge of the sheet, where a solar cell is positioned. Due to the long path length in the sheet before reaching the solar cell, re-absorption and re-emission mechanisms play an important role in LSCs [17–21].

However, when more complex optical designs are considered, programming of true Monte Carlo algorithms becomes impractical because complex ray tracing intersection algorithms require a huge programming effort. In these situations, commercial ray tracers offer a useful solution. This type of software handles the simulation of light propagation phenomena such as surface scattering, bulk scattering, and Snell's and Fresnel's laws, and the generation of desired output quantities such as transmitted spectra, radiation patterns, and radiance maps allows for straight forward analysis.

Some commercial ray tracers, such as LightTools and Radiant Zemax, offer a complete wavelength conversion functionality, and handle luminescence very similar to the above described true Monte Carlo algorithms. These ray tracers allow for full spectrum simulations including simulations of luminescent cascade systems and materials with a strong overlap between excitation and emission spectra.

Other commercial ray tracers, such as TracePro, ASAP, and FRED, offer a limited wavelength conversion functionality, which is based on the conversion of ray sets, rather than true Monte Carlo luminescence algorithms where each ray or photon is treated individually. This approach is well suited for a two wavelength approach, where one wavelength represents the excitation and another wavelength represents the emission by the luminescent material. This two wavelength approach is useful and gives adequate results for many applications [24–28]. However, this method does not allow the simulation of re-absorption and re-emission events in the material, and consequently it will not lead to accurate results for luminescent cascade systems or for materials showing an overlap between excitation and emission spectra.

To allow for full spectrum simulations of complex optical systems incorporating luminescent cascade systems or luminescent components with a significant overlap between excitation and emission spectra using commercial software with limited wavelength conversion functionality, a hybrid ray tracing technique is presented. This method combines the strengths of commercial ray tracing software with a programming tool for the modeling of complex luminescent processes.

2. Algorithm for the hybrid ray tracing tool

In true Monte Carlo algorithms, a ray or photon is emitted by a source and traced through the optical system, applying the appropriate probability functions at interfaces and in the media, until the ray or photon is absorbed, escapes the system, or reaches the desired target [17–21]. In luminescent media, a photon can be absorbed and a new photon can be emitted with a longer wavelength, with a probability equal to the quantum efficiency of the medium. This photon can be treated as any other photon and the absorption and re-emission process can occur multiple times. This allows for adequate modeling of luminescent cascade systems and luminescent materials with a significant overlap between excitation and emission spectra.

In the hybrid tool, switching between ray tracer and programming tool for each individual ray would require a large number of interactions between both programs, creating a large overhead, reducing the efficiency of the hybrid algorithms and increasing the computation time. It would thus be efficient to convert the true Monte Carlo algorithms for luminescent materials, treating each ray or photon individually, to an approach treating ray sets.

To allow the implementation of the hybrid method, the ray tracer must satisfy the following requirements: (1) users must be able to send commands from the programming tool to the ray tracer; (2) the ray tracing software must allow the saving of volumetric absorption distribution for each wavelength; (3) the ray tracer must allow the insertion of a source based on a random ray set defined by the user. Most commercial non-sequential ray tracers satisfy these three requirements.

In Fig. 1, the algorithm for the hybrid method is presented. The method starts with the shortest wavelength. If a selected wavelength occurs within the spectrum of a source, a ray set

#217365 - $15.00 USD Received 18 Jul 2014; revised 20 Sep 2014; accepted 23 Sep 2014; published 30 Sep 2014

is attributed to the source(s), which is traced through the simulation geometry. The ray tracer tracks the rays until they are absorbed, escape the model, or reach a predefined target.

If any absorption in luminescent components occurs, i.e. when the selected wavelength falls within the excitation wavelength region, the absorption is stored as a volumetric absorption distribution (VAD). Next, the desired information, such as transmitted flux, radiation pattern, or radiance maps, is stored.

If the current selected wavelength is present in the emission spectra of (one of) the luminescent material(s), a volumetric emission distribution (VED) is generated, based on the previously stored VADs. A more thorough discussion on how the VED is generated can be found in section 3.

Next, a ray set is attributed to the luminescent component(s), based on the VED and traced through the system. If this emission wavelength is also an excitation wavelength of (one of) the luminescent component(s), the absorption is stored as a VAD Again, the desired output information is gathered and stored.

Finally, the algorithm selects the next wavelength and the previous steps are repeated, until all wavelengths have been traced.

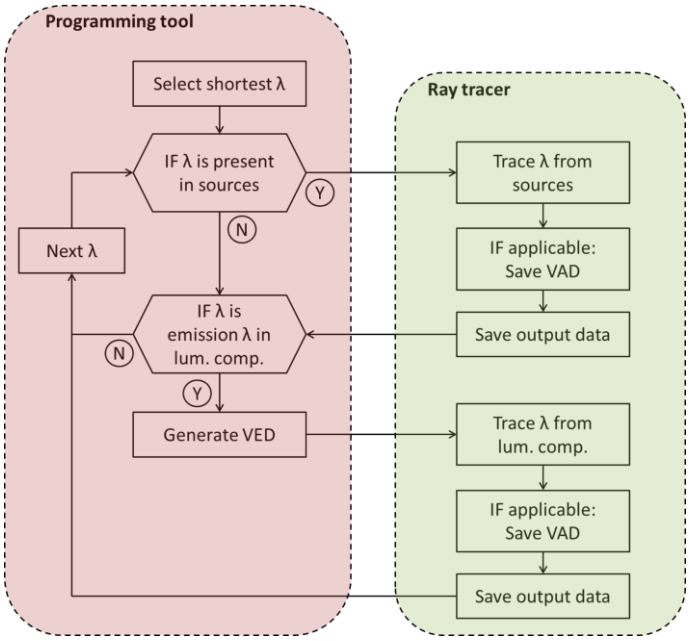

Fig. 1. Flowchart of the hybrid ray tracing algorithm. VAD and VED stand for volumetric absorption and emission distribution, respectively.

It should be noted that the presented algorithms only allow for down-conversion. They can be converted for up-conversion, by reversing the order in which the wavelengths are handled, i.e. from long to short wavelengths instead of short to long. With these algorithms it is not possible to treat both down- and up-conversion in the same simulation.

3. Generation of a volumetric emission distribution

One of the difficulties of the hybrid algorithm is the generation of the VEDs. The ray set representing the emission from the luminescent component at emission wavelength λ_M is determined by all the excitation wavelengths shorter than the emission wavelength, schematically represented in Fig. 2.

In the VADs, the position (‘pos’) and absorbed flux (‘flux’) for each absorption event are stored in a table (Fig. 2). The number of absorption events depends on how the ray tracer treats absorption. If a ray is either completely absorbed or not absorbed with a certain

#217365 - $15.00 USD Received 18 Jul 2014; revised 20 Sep 2014; accepted 23 Sep 2014; published 30 Sep 2014

probability, the maximum number of absorption events is equal to the number of rays attributed to the sources. If the ray tracer uses a voxelized approach, where the luminescent volume is subdivided into a user defined number of smaller volumes (voxels), and the absorption per voxel is stored, the maximum number of absorption events will be equal to the number of voxels used in the simulation. However, if the ray tracer allows partial absorption of the rays (i.e. the ray tracer decreases the flux attributed to the ray after each absorption event), and no voxels are used, the number of absorption events can become several magnitudes larger than the number of rays attributed to the sources in the simulation, resulting in a very large VAD table.

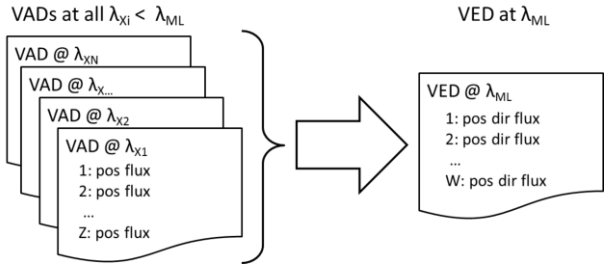

Fig. 2. Schematic representation of information in the volumetric absorption distributions (VAD) and the volumetric emission distributions (VED). "Pos" stands for position, and "dir" stands for direction.

In the VEDs, the position ('pos'), emission direction ('dir'), and emitted flux ('flux') are stored as a table (see Fig. 2). For each excitation or emission wavelength a corresponding VAD or VED is created, respectively.

The conversion from several VADs at excitation wavelengths λ_{Xi} to a VED at emission wavelength λ_M can be done in several ways. The first option is to generate an emission event in the VED for each absorption event. However, from Fig. 2, it can be seen that the VADs at all excitation wavelengths must be combined, leading to a large number of absorption events, and computation time would rise considerably. Moreover, if the ray tracer partially absorbs the rays, the number of absorption events will even higher.

The alternative is to create only a limited number of emission events (typically equal to the number of rays per wavelength attributed to the source(s)). In this paper, two methods to create VEDs are discussed. The first method is based on a random selection of absorption events to generate emission events, and is referred to as the 'random approach'. The second method combines multiple absorption events which are spatially close to each other, to generate emission events. This method is referred to as the 'combined approach'.

3.1 Energy balance

To convert absorption events into emission events, the absorbed flux must be appropriately converted to the emitted flux. To calculate the emitted flux at emission wavelength λ_M, ($\Phi_{em}(\lambda_M)$) from the absorbed fluxes at excitation wavelengths λ_{Xi}, ($\Phi_{abs}(\lambda_{Xi})$), the quantum efficiency and energy losses due to the Stokes shift must be taken into account. In Eq. (1), the power flux conversion for a single photoluminescent material is given.

$$\Phi_{em}(\lambda_M) = \int \Phi_{abs}(\lambda_{Xi}).w_M(\lambda_M, \lambda_{Xi}).QE(\lambda_{Xi}).\frac{\lambda_{Xi}}{\int w_M(\lambda_M, \lambda_{Xi}).\lambda_M .d\lambda_M}.d\lambda_{Xi} \qquad (1)$$

Where $QE(\lambda_{Xi})$ represents the quantum efficiency. The absorbed flux at one excitation wavelength will result in emission at multiple emission wavelengths according to the emission spectrum: only a fraction of the emitted light will be emitted at the particular emission wavelength λ_M. In Eq. (1), the weight $w_M(\lambda_M,\lambda_{Xi})$ is introduced to represent the fraction of the converted flux emitted at wavelength λ_M due the absorption at excitation wavelength λ_{Xi}. This weight can be immediately derived from the emission spectrum, and is

#217365 - $15.00 USD Received 18 Jul 2014; revised 20 Sep 2014; accepted 23 Sep 2014; published 30 Sep 2014

normalized to satisfy $\int w_M(\lambda_M, \lambda_{Xi}).d\lambda_M = 1$. The fraction in Eq. (1) represents the energy loss due to the Stokes shift.

When multiple photoluminescent materials are combined, each with their proper *QE*, absorption and emission spectra, the emitted flux can be calculated from Eq. (2).

$$\Phi_{em}(\lambda_M) = \sum_{j=1}^{R} \int \Phi_{abs}(\lambda_{Xi}).w_{X,j}(\lambda_{Xi}).w_{M,j}(\lambda_M, \lambda_{Xi}).QE_j(\lambda_{Xi}).\frac{\lambda_{Xi}}{\int w_{M,1}(\lambda_M, \lambda_{Xi}).\lambda_M.d\lambda_M}.d\lambda_{Xi} \quad (2)$$

In Eq. (2), the subscript *j* refers the optical properties of the *R* different photoluminescent materials combined in the photoluminescent component. A new weight factor $w_{X,j}(\lambda_{Xi})$ represents the fraction absorbed by the particular photoluminescent material *j* and can be calculated using Eq. (3).

$$w_{X,j}(\lambda_{Xi}) = \frac{\mu_{a,j}(\lambda_{Xi})}{\mu_{a,1}(\lambda_{Xi}) + \mu_{a,2}(\lambda_{Xi}) + ... + \mu_{a,R}(\lambda_{Xi})} \quad (3)$$

Herein, $\mu_{a,j}(\lambda_{Xi})$ represents the absorption coefficient of photoluminescent material *j*, which is the average distance a photon or ray can travel through the photoluminescent material before being absorbed. This quantity is dependent on the concentration of the absorbing material used in the luminescent component.

3.2 Random approach

A first way to generate a VED at an emission wavelength is to randomly select absorption events from the various VADs and appropriately convert them to emission events. A schematic flowchart of the random approach to convert VADs to a VED is given in Fig. 3 (a). To ensure the energy balance of the wavelength conversion process is correct, the total absorbed flux at each excitation wavelength must be known or calculated from the VAD. From each VAD for which the wavelength contributes to the emission at the particular emission wavelength, a number of absorption events are randomly selected. The number of selected events per VAD is weighted by the contribution to the emission at wavelength λ_M. This way, wavelengths with strong absorption are represented by more absorption events than wavelengths with weak absorption.

Next, the fluxes of the selected absorption events per excitation wavelength are scaled such that the sum of these fluxes agree with the total absorbed flux at that excitation wavelength. This ensures a correct energy balance for the simulations. Finally, the absorbed fluxes are converted according to Eq. (1) or (2) and a random direction is attributed to the emission event.

Due to the random selection of the absorption events, additional noise will be introduced in the simulations.

3.3 Combined approach

A second way to create a VED from the various VADs, is to combine multiple absorption events to create one emission event. A schematic flowchart of the combined approach is given in Fig. 3(b). In this approach, the first step is to convert all the absorbed fluxes to the emitted flux at the selected emission wavelength λ_{ML} according to Eq. (1) or (2). Next, all absorption events of the various VADs are combined in one large table. A sorting algorithm now searches for absorption events which are spatially close to each other.

Next, a fixed number of absorption events that are located close to each other are combined: the corresponding emission flux is summed, an average position is determined from the positions of the various absorption events, and a random direction is attributed to the new emission event. The fixed number of absorption events is equal to the total number of absorption events divided by the desired number of emission events.

#217365 - $15.00 USD Received 18 Jul 2014; revised 20 Sep 2014; accepted 23 Sep 2014; published 30 Sep 2014

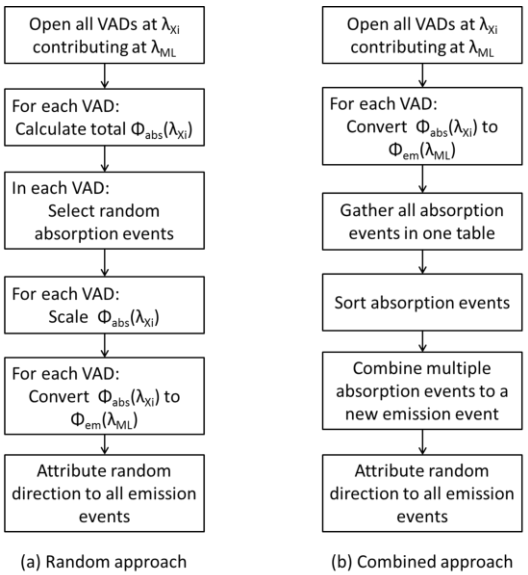

Fig. 3. Flowchart of the two approaches for the conversion of volumetric absorption distributions (VADs) to a volumetric emission distribution (VED): (a) the random approach, and (b) the combined approach.

The sorting algorithm required in this approach can be time consuming (especially for a large number of absorption events), which can reduce the efficiency. This step is however essential, since omission would cause all emission events to take place close to the center of the luminescent component.

The advantage of the combined approach is that less noise will be introduced in the simulation compared to the 'random approach', since all available absorption information is used, rather than only a number of random absorption events.

4. Validation

The hybrid ray tracing method was validated by applying the method to a simple luminescent cascade system with simple geometry. The system allowed for the analytical calculation of the emitted luminescent fluxes which were then compared with the simulation results. In the simulations, three wavelengths were considered: 450 nm (blue), 550 nm (green), and 650 nm (red). The geometry consisted of a square source (0.5x0.5 mm2) and a cube (1x1x1 mm3), and is presented in Fig. 4. The source emitted a blue flux (Φ_{source} = 1W) perpendicular on one of the sides of the cube. The cube contained two luminescent non-scattering pigments, the properties of which are given in Table 1. The first material absorbed blue and emitted green, the second material absorbed green and emitted red: together they constituted a luminescent cascade system. The quantum efficiency of the materials was 0.9 and 0.8, respectively. The refractive index of the cube was set to 1, to avoid Fresnel reflections. A hollow sphere was positioned around the geometry as detector to capture all rays escaping the cube.

The output data of the simulation was the spectral radiant flux escaping the simple geometry (Φ_{det}), the detected radiant fluxes are presented in Table 1. The simulation results were obtained using 100 000 rays per wavelength. Both approaches for the conversion of VADs to VEDs returned the same result.

The flux transmitted (Φ_T) through the cube can be calculated according the Beer-Lambert law, Eq. (4).

$$\Phi_T = \Phi_{source}.\exp(-\mu_a.d) \tag{4}$$

With d is the path length of the light travelling through the cube. At 450 nm, μ_a = 1 mm^{-1} and d = 1 mm, resulting in a transmitted flux of 0.37 W, which was in agreement with the

#217365 - $15.00 USD Received 18 Jul 2014; revised 20 Sep 2014; accepted 23 Sep 2014; published 30 Sep 2014

simulation result (see Table 1). The flux was absorbed by the first luminescent material and amounted to 0.63 W. This material converted the light from 450 to 550 nm, with QE = 0.9, the emitted flux was thus 0.47 W. Part of the flux emitted at 550 nm was re-absorbed by the second luminescent component and converted to 650 nm.

Table 1. Optical properties and simulations result, μ_a and w_M are the absorption coefficients and emission weights, $\Phi_{scource}$ and Φ_{det} are the flux emitted by the source and captured by the detector.

λ (nm)	450	550	650
Φ_{source} [W]	1	0	0
$\mu_{a,1}$ [mm^{-1}]	1	0	0
$\mu_{a,2}$ [mm^{-1}]	0	0.5	0
$w_{M,1}$	0	1	0
$w_{M,2}$	0	0	1
Φ_{det} [W]	0.37	0.36	0.07

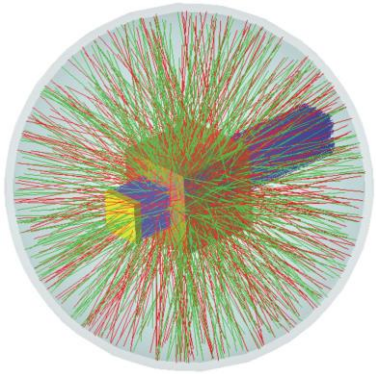

Fig. 4. Geometry used for the validation. The yellow square represents the source, emitting blue rays perpendicular onto one of the sides of the orange cube, containing the luminescent particles. The hollow sphere (gray) acts as detector and captures all rays escaping the cube.

The average distance the re-emitted rays travelled through the cube could be approximated as 0.5 mm. The part of the re-emitted flux escaping the luminescent cube before re-absorption was calculated using Eq. (4), with d = 0.5 mm, and μ_a = 0.5 mm^{-1}. This resulted in Φ_{det} = 0.36 W at 550 nm, which was in agreement with the simulation result.

Finally, the absorbed flux at 550 nm (which amounted to 0.10 W) was converted to 650 nm with QE of 0.8. The emitted flux at 650 nm amounted to 0.07 W, again in agreement with the simulation result. It can be concluded that the presented hybrid ray tracing algorithms indeed successfully handle the wavelength conversion in a luminescent cascade system.

5. Application: remote phosphor LED module

An illustrative ray trace simulation of a remote phosphor light-emitting diode (LED) module was performed. The simulation results from the hybrid ray tracer and a commercial ray tracer implementing true Monte Carlo algorithms and the performance of the random and combined approach to create VEDs were compared.

The (virtual) LED module consisted of a cylindrical cavity (inner diameter 74 mm, height 40 mm), with six blue LEDs mounted on the base plate, each emitting a radiant flux of 2 W, similar to the module described by Acuna *et al.* [28] The cavity was attributed a lambertian reflection pattern with reflectance of 0.98. A remote phosphor converter (RPC) was positioned on top of the cavity (thickness 2 mm). A schematic representation of the LED module is given in Fig. 5(a).

The virtual RPC model used in this study consisted of a PMMA matrix material (refractive index 1.5) in which YAG:Ce phosphor and CIS/ZnS quantum dots were mixed. The YAG:Ce phosphor emitted yellowish light, the quantum dots emitted reddish light. The

#217365 - $15.00 USD Received 18 Jul 2014; revised 20 Sep 2014; accepted 23 Sep 2014; published 30 Sep 2014

emission and absorption spectra of the luminescent materials are presented in Fig. 5(b), together with the emission spectrum of the blue LEDs.

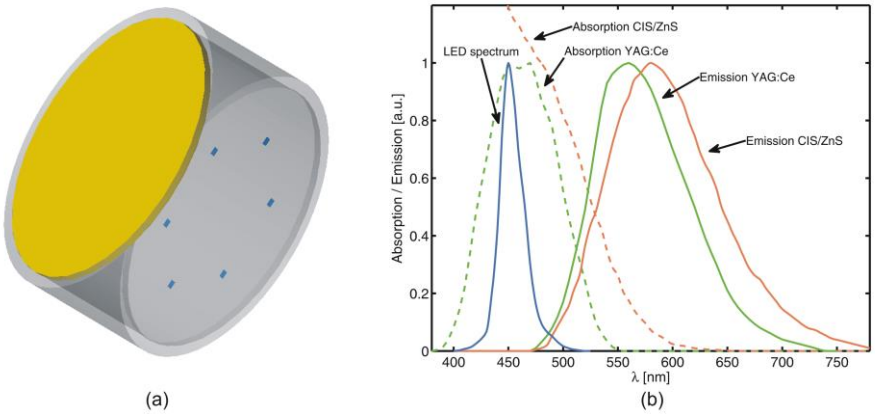

Fig. 5. Schematic representation of the remote phosphor LED module (a), and the absorption and emission spectra of the luminescent materials used for the remote phosphor converter and the blue LEDs (b).

The absorption, emission and scattering properties of the YAG:Ce phosphor were taken from the work of Liu *et al*. [29] The absorption and emission properties of the CIS/ZnS quantum dots were taken from the work of Song *et al*. [30] Due to their small size, scattering caused by the quantum dots could be neglected. The concentration of the YAG:Ce phosphor and the quantum dots was optimized to obtain a LED module with a correlated colour temperature (CCT) of 3000 K. From Fig. 5(b), it can be seen that the absorption spectrum of the CIS/ZnS quantum dots largely overlaps the emission spectrum of the YAG:Ce phosphor. The combination of both luminescent particles thus created a luminescent cascade system, moreover, an overlap between the excitation and emission spectra of both luminescent materials was present.

The hybrid method as presented in this paper was implemented using the commercial ray tracer TracePro 7.3 and Matlab 7.1 as programming tool. For all simulations, the maximum number of emission events for each emission wavelength was set to be equal to the number of rays per wavelength set for the sources in the simulation.

5.1 Hybrid ray tracer vs true Monte Carlo

The simulation results of the remote phosphor LED module obtained from the presented hybrid ray tracing technique are compared to the results obtained from a true Monte Carlo ray tracer (LightTools). The total spectral radiant flux emitted by the remote phosphor LED module as obtained from both ray tracers is shown in Fig. 6.

#217365 - $15.00 USD Received 18 Jul 2014; revised 20 Sep 2014; accepted 23 Sep 2014; published 30 Sep 2014

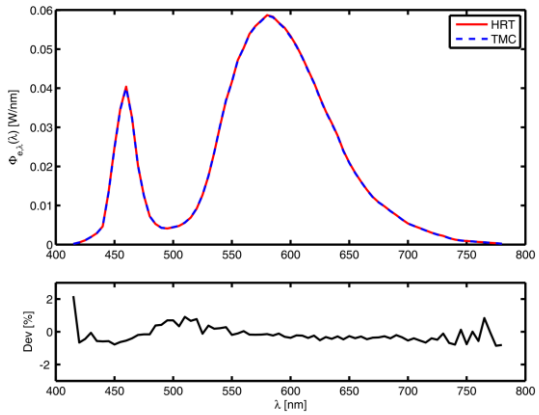

Fig. 6. The spectral radiant flux of the remote phosphor LED module obtained from the presented hybrid ray tracer (HRT) and a true Monte Carlo (TMC) ray tracer, together with the deviation between both spectra.

An excellent agreement between the results obtained from both ray tracers can be observed. The normalized RMS deviation is smaller than 0.5% and can be attributed to noise in the simulations.

5.2 Random vs combined approach

The remote phosphor LED module was also used as test case to investigate the required number of rays to achieve sufficient accuracy for both VED generation strategies was investigated. This allowed for the selection of the most efficient approach.

In principle, using an infinite number of rays (and thus infinite computation time), a ray tracing simulation would provide the perfect solution for the light propagation problem. Using a finite number of rays will decrease the required computation time but will introduce noise in the results.

In Fig. 7, the simulated total spectral radiant flux emitted by the remote phosphor LED module is presented for both the 'random' and the 'combined' approach using 1000 rays per wavelength. The simulations were performed in wavelength steps of 5 nm in the visible wavelength range (380 nm –780 nm). It can be observed that the results obtained with the random approach are more noisy compared to the results obtained with the combined approach, which is in agreement with the prediction formulated in section 3.

The accuracy of the ray tracing simulations was determined as a function of the number of rays per wavelength used in the simulations. For each number of rays/wavelength, 5 subsequent simulations were performed, with different random ray sets for each wavelength. The relative standard deviation on the spectral radiant flux, averaged over 41 wavelengths, was used as a measure of the accuracy.

The results are presented in Fig. 8(a). It is obvious that the random approach generates more noise compared to the combined approach. If the desired accuracy on the spectral radiant flux is at least 1%, the random approach requires 20 000 rays per wavelength, while the combined approach requires only 5000 rays per wavelength.

#217365 - $15.00 USD Received 18 Jul 2014; revised 20 Sep 2014; accepted 23 Sep 2014; published 30 Sep 2014

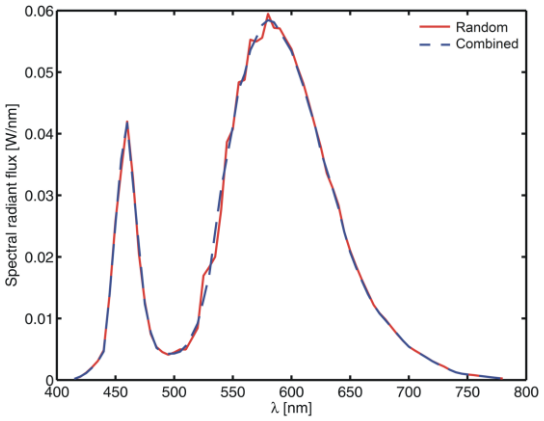

Fig. 7. The simulated spectral radiant flux of the remote phosphor LED module obtained with the random and combined approach, using 1000 rays per wavelength for the simulations.

The computation time of both approaches was also compared, by taking the average computation time of the 5 subsequent traces performed to determine the accuracy. All simulations were run on the same PC, with a Pentium Dual Core CPU E5700 3 GHz with 8 GB RAM memory. The operating system was Windows 7 64bit Professional. In Fig. 8(b), the computation time of both approaches is presented as a function of the number of rays per wavelength.

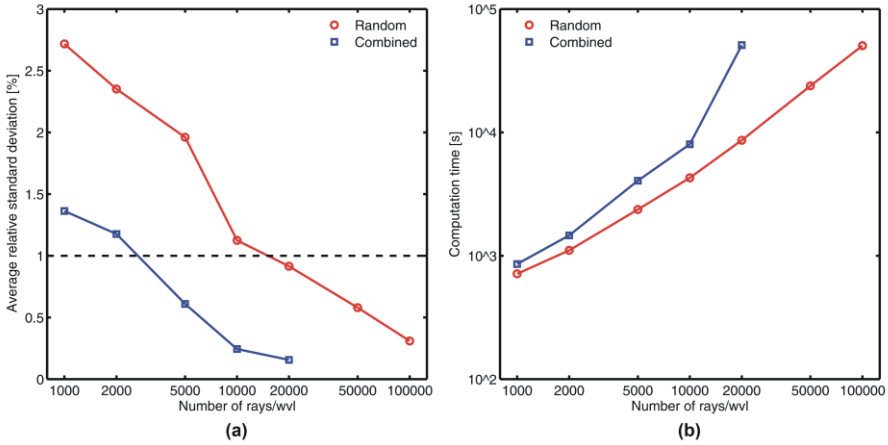

Fig. 8. The average relative standard deviation of the simulated spectral radiant flux using the random and combined approach (a), and the corresponding computation time (b). The dashed black line denotes the desired maximum average relative standard deviation threshold of 1%.

From Fig. 8(b), it is obvious that the combined approach requires more computation time for the same number of rays per wavelength. This is expected, since the combined approach requires a time consuming sorting algorithm. The computation time for the random approach increases approximately linear with the number of rays per wavelength. For the combined approach however, the computation time increases faster than linear as a function of the number of rays per wavelength, due to the fact that the number of computations for the sorting algorithm as a function of the number of elements to sort increases faster than linear.

Considering the desired maximum average relative standard deviation of 1%, the computation time for the random approach amounted to 2.4 hours (using 20 000 rays per wavelength) and amounted to 1.1 hours for the combined approach (using 5000 rays per

#217365 - $15.00 USD Received 18 Jul 2014; revised 20 Sep 2014; accepted 23 Sep 2014; published 30 Sep 2014

wavelength). The combined approach is thus the most efficient way to obtain simulation results with a predefined accuracy.

5. Conclusion

A hybrid ray tracing algorithm, combining a commercial ray tracer and a programming tool was presented for the adequate modeling of luminescent cascade systems. This method has the advantage that it combines the strengths of the ray tracer with adequate modeling of luminescent behavior. The use of a commercial ray tracer allows for the implementation of complex designs the simulation of light propagation phenomena such as surface scattering, bulk scattering, Snell's and Fresnel's laws…, and allows for straight forward generation of output quantities such as transmitted spectra, radiation patterns, radiance maps… The programming tool takes care of the luminescent conversion processes. The hybrid ray tracing tool offers an adequate solution for the modeling of a luminescent cascade system in complex designs, which only requires limited programming effort.

In the presented hybrid method, wavelength conversion is handled by converting volumetric absorption distributions (VADs) into volumetric emission distributions (VEDs). Due to the large amount of absorption events in the VAD, it is not feasible to generate an emission event for each absorption event. Two approaches to create a reasonable number of emission events were investigated: a random approach where absorption events were randomly selected to create emission events, and a combined approach where multiple absorption events were combined to create one emission event.

A virtual remote phosphor LED module was used as an illustration of the use of the hybrid ray tracing tool. The simulation results obtained from the hybrid ray tracer and a commercial ray tracer implementing the wavelength conversion on a ray by ray basis showed an excellent agreement with a normalized RMS deviation less than 0.5%.

Using the LED module as test case, it was found that the random approach is less accurate but faster compared to the combined approach using the same number of rays per wavelength. Setting the desired maximum average relative standard deviation for the spectral radiant flux of the LED module to 1%, it was found that the combined approach achieves the desired accuracy in approximately half the time of the random approach.

Due to the fact that the combined approach requires a sorting algorithm, the computation time increases faster than linear. If a large number of rays are required, e.g. to calculate radiation patterns or radiance maps, it is beneficial to perform the simulation with the combined approach with a limited number of rays per wavelength multiple times with different random ray sets attributed to the sources, and subsequent combination of the results to reduce the noise.

Acknowledgments

The authors would like to thank the SIM (Flemish Strategic Initiative for Materials) and IWT (Flemish agency for Innovation by Science and Technology) for their financial support through the SIM-IWT ICON project 'Solcap' (IWT 100733).